

# Pump radiation distribution in multi-element first cladding laser fibres

M.A. Mel'kumov, I.A. Bufetov, M.M. Bubnov,  
A.V. Shubin, S.L. Semenov, E.M. Dianov

**Abstract.** Pump radiation transfer is studied experimentally in multi-element first cladding laser fibres. A model of this process is proposed, which is in good agreement with experimental results. An all-fibre single-mode cw ytterbium laser based on a three-element first cladding fibre with an output power of 100 W is fabricated.

**Keywords:** fibre laser, double-clad fibre, ytterbium.

## 1. Introduction

The output power of single-mode fibre lasers was increased in the last years by more than an order of magnitude, from 110 W in 1999 [1] to 1.4 kW in 2005 [2]. Comparable power levels ( $\sim 300$  W) were obtained in lasers with linearly polarised radiation [3] and single-frequency lasers [4]. This was achieved mainly due to the development of diode-pump systems and the improvement of characteristics of laser fibres with a large mode-field diameter. In addition, the use of new pump schemes also plays an important role in the increase in the output power of single-mode fibre lasers.

At present, the following pump radiation coupling methods are used in the highest-power single-mode fibre lasers:

(i) Direct pump radiation coupling through the end face of a double-clad fibre. In this case, the second end face of the fibre serves to couple out laser radiation [5]. Laser radiation can be also coupled through the both ends of a double-clad laser fibre [6], thereby doubling the coupled power and increasing the output power of the laser. However, the use of both fibre ends for pump radiation coupling requires the employment of non-fibre elements such as lenses and multilayer dielectric mirrors, which severely complicates the laser design and reduces its reliability.

(ii) Pump radiation coupling through the fibre ends by means of multimode couplers [7–9]. Such devices have several multimode inputs and one multimode output with a

larger aperture and a large diameter than for input fibres and consist of a few fibres spliced into one. Commercial devices have low losses; however, they do not withstand high powers (the limitation is 20 W for each input) and considerably (more than by half) reduce the radiation brightness.

(iii) Pump radiation coupling by using a double-clad fibre, in which, unlike coupling method (i), the first cladding consists of several individual fibres (Fig. 1) in optical contact with each other [10]. These are the so-called multi-element first cladding (MFC) fibres (which are usually called GTWave fibres in papers in English) [11].

In addition, the combination of the second and third radiation coupling methods can be used in some cases.

At present, the maximum output power was achieved in fibre lasers with pump radiation coupling using method (i) [2]. Nevertheless, it seems that all-fibre coupling methods (ii) and (iii) are more promising for most applications because, unlike methods with lenses, they do not require any adjustment, much more stable with respect to external perturbations (especially vibrations and temperature variations) and are potentially more durable.

MFC fibre lasers are also attractive because they allow one to increase rather simply by several times the pump power coupled into the laser fibre by increasing the number of pump stages (see below). However, in this case, contradictory requirements to the fibre length appear. On the one hand, the laser fibre length between the two successive sites of pump radiation coupling should be sufficiently large to provide almost complete absorption of pump radiation by active ions. On the other hand, the total laser length should be as small as possible to increase the threshold of various nonlinear effects (SRS, SBS, etc.) restricting the output power of the laser (for this purpose, the mode-field diameter in laser fibres is also increased). To reduce the absorption length of pump radiation from the first cladding, the amount of absorbing ions per the unit length in the laser fibre core is increased (up to the value admitted by the technology and conditions of formation of the waveguide structure in the fibre). However, the increase in the absorption coefficient for pump radiation from the first cladding in MFC fibres is expedient only when the fibre length at which the pump power densities in individual MFC fibres are equalised is small compared to the pump absorption length.

Although MFC fibre systems have been studied in a number of recent papers [10–12, 15], the pump radiation transfer between individual components of MFC fibres has not been considered so far.

---

M.A. Mel'kumov, I.A. Bufetov, M.M. Bubnov, A.V. Shubin, S.L. Semenov, E.M. Dianov Fiber Optics Research Center, A.M. Prokhorov General Physics Institute, Russian Academy of Sciences, ul. Vavilova 38, 119991 Moscow, Russia; e-mail: melkoumov@fo.gpi.ru, iabuf@fo.gpi.ru

Received 19 July 2005

Kvantovaya Elektronika 35 (11) 996–1002 (2005)

Translated by M.N. Sapozhnikov

---

In this paper, we studied experimentally the properties of two-element first cladding fibres fabricated at the FORC RAN and proposed a model describing power transfer between the elements in such fibres. The possibility of increasing the output power of MFC fibre lasers and the problems involved in this case were demonstrated by the example of a 100-W cw ytterbium laser.

## 2. Output power scaling for MFC fibre lasers

An MFC fibre consists of a single-mode active fibre in optical contact with one or more parallel multimode silica fibres, which are surrounded by a cladding with the refractive index that is slightly lower than that of silica (Fig. 1). The active fibre core is doped with rare-earth ions, while passive fibres are coreless and made of pure silica glass. Passive multimode fibres to which the pump radiation is coupled are in optical contact with the active fibre over their entire length to provide energy transfer to the latter. All the fibres are optically coupled with each other and represent in fact the first cladding for the active fibre core.

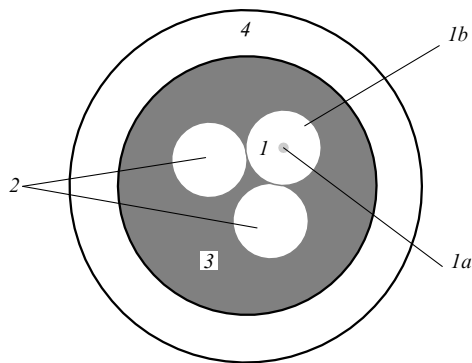


**Figure 1.** Cross section of a three-element MFC fibre: (1) active fibre [(1a) core; (1b) first cladding]; (2) passive fibres; (3) common cladding with a lower refractive index; (4) protective jacket.

An important advantage of MFC fibres over conventional double-clad fibres is the initially asymmetric geometry of their cross section (see Fig. 1). As a result, unlike conventional double-clad fibres, in which, as a rule, the non-cylindrical (square, rectangular, hexagonal, D-like, etc.) shape of the first-cladding cross section should be used to provide the efficient absorption of all the pump radiation modes in the fibre core [13, 14], the cross sections of active and passive fibres in MFC fibres can be circular. This considerably simplifies fibre splicing and reduces losses in splices of the active fibre with other single-mode fibres.

Because different multimode fibres in an MFC fibre are not mechanically coupled with each other (being only surrounded by a polymer cladding), they can be separated if necessary, and passive fibres can be independently coupled with pump sources and active fibres spliced with single-mode fibres for coupling and coupling out signal radiation. The structure of MFC fibres allows one to assemble both all-fibre lasers, by splicing single-mode fibres with fibre Bragg gratings (FBGs) to the ends of the active fibre, and fibre amplifiers, providing a convenient access to both outputs of the amplifying fibre. Fibre systems assembled from fibres of such type can have several sites

for pump coupling, which permits the summation of the pump powers coupled at different sites, thereby constructing high-power fibre lasers.

A 50-W single-mode laser based on a three-element fibre of this type was fabricated in [10]. To increase the output power up to 100 W, we used two series-connected pump schemes for a 50-W laser to double the pump power (Fig. 2). As a result, the number of sites for pump radiation coupling doubled to eight.

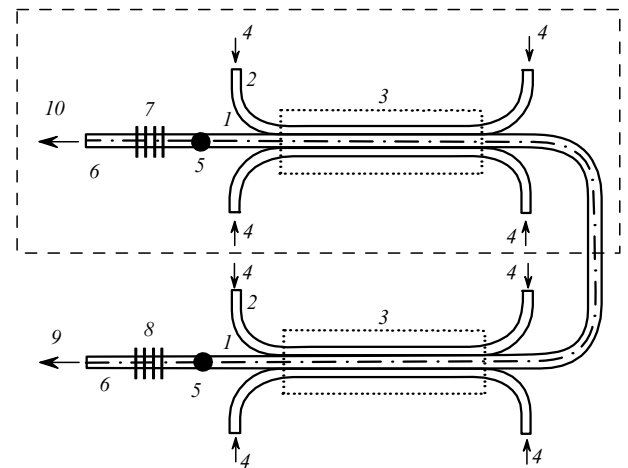


**Figure 2.** Scheme of a 100-W three-element MFC fibre laser (scheme of a 50-W laser is distinguished by dashed straight lines [10]): (1) active fibre; (2) passive fibres; (3) polymer cladding with a low refractive index; (4) pump radiation; (5) splices of the signal fibre with fibres (6) in which FBGs are written; (7) highly reflecting FBG; (8) FBG at the output end of the laser with the reflectivity  $\approx 5\%$ ; (9) output radiation of the laser; (10) laser radiation transmitted through the highly reflecting FBG.

This pump scheme was realised by removing a polymer cladding and cutting passive fibres in the middle of a three-element fibre piece. The active fibre remained intact and the cavity was still formed by a pair of FBGs connected to its ends. The length of each of the two parts of the laser obtained in this way was chosen to provide the pump radiation absorption no less than 10 dB. It was taken into account that the width of the pump line of laser diodes is comparable to that of the absorption peak and the maximum of the pump spectrum shifts depending on the pump power.

Pumping was performed by eight 20-W laser-diode modules (MILON laser, St. Petersburg) emitting at the wavelength changing between 963 and 978 nm depending on the output power due to the absence of thermal stabilisation.

The laser cavity consisted of a highly reflecting ( $\sim 100\%$ ) FBG and output FBG with the reflectivity 5%. FBGs were written in the fibre core with the cut-off wavelength of the fundamental mode near  $1\ \mu\text{m}$ . The maximum of the FBG reflection was at  $1.068\ \mu\text{m}$ . The active fibre core was made of a phosphosilicate glass [15] doped with  $\text{Yb}^{3+}$  ions at a weight concentration of  $\sim 2\%$ . The total length of the active fibre was 44 m ( $2 \times 22$  m).

Figure 3 shows the dependence of the output power of the laser on the pump power. To develop a 100-W laser, we fabricated a three-element MFC fibre with parameters substantially different from those of the fibre used in the

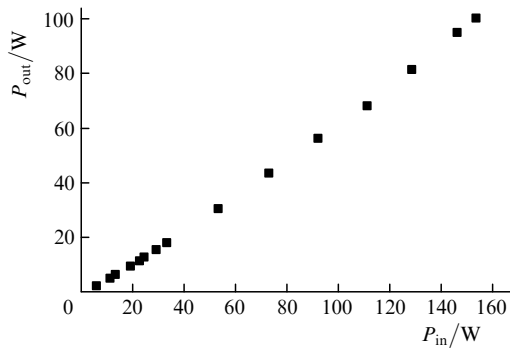


**Figure 3.** Dependence of the output laser power  $P_{out}$  on the coupled pump power  $P_{in}$ .

50-W laser [10]. The diameter of the laser radiation mode in the active fibre was increased up to  $14.5 \mu\text{m}$  (from  $8 \mu\text{m}$ ), the absorption coefficient  $\alpha_{clad}$  from the first cladding at  $975 \text{ nm}$  increased up to  $1.7 \text{ dB m}^{-1}$  (compared to  $0.9 \text{ dB m}^{-1}$  in [10]). This allowed us to reduce the absorption length of pump radiation and to decrease the required length of the laser fibre.

Due to such changes in the laser design, the threshold power of nonlinear effects such as SRS and SBS proved to be higher than the maximum output power of the laser, which is confirmed by a linear dependence of the output power on the pump power presented in Fig. 3. In addition, the increase in the fundamental mode field diameter substantially reduced power losses due to the broadening of the laser emission spectrum caused by four-photon mixing.

Upon scaling the output power of the laser to even greater values in order to suppress nonlinear effects, it is necessary along with other measures to decrease further the pump radiation absorption length in the MFC fibre. However, there exists another factor, which can restrict a decrease in the laser fibre length and, therefore, the maximum achievable output power of a fibre laser. This is the efficiency of pump radiation transfer between individual elements of the fibre.

The efficiency of radiation energy transfer is usually described by *the coupling coefficient or the coupling length* [17]. In this paper, we will call the coupling length  $L_c$  the length of an MFC fibre at which the radiation intensities in the active and passive fibres become virtually equal when the radiation is coupled only to one of them. Note that a small coupling length is required not only to provide a rapid transfer of the pump radiation from the passive fibre to the active one but also for the efficient redistribution of energy between the beams intersecting and not intersecting the active fibre core. The latter is necessary for absorption of all the beams propagating in the first cladding in the fibre core, including those that have not initially intersected the core.

### 3. Model for calculating the coupling length in MFC fibres

Radiation transfer between closely spaced waveguides is often described by using the wave analysis of the modes of optically coupled waveguides [16, 17]. This is convenient in the case of waveguides with a moderate number of guided modes. Multimode fibres with the first-cladding diameter  $D_{in} = 80 - 300 \mu\text{m}$  and the numerical aperture  $\text{NA} = 0.2 -$

$0.4$  have a very large number of modes, and so their mode description is quite complicated. At the same time, it is well known [17] that in this case the ray approximation is valid, which we will use below to describe the power transfer from one element of the MFC fibre to another.

Figure 4 shows the cross section of a two-element MFC fibre. Hereafter, we assume for simplicity that passive (I) and active (II) fibres have equal diameters. The minimal distance between the boundaries of fibres is denoted by  $d$  (we assume for generality that the elements of the MFC structure do not touch each other, which can be caused by the imperfection of manufacturing technology of such fibres). The plane in which the axes of both fibres lie is denoted by  $\tau$ .

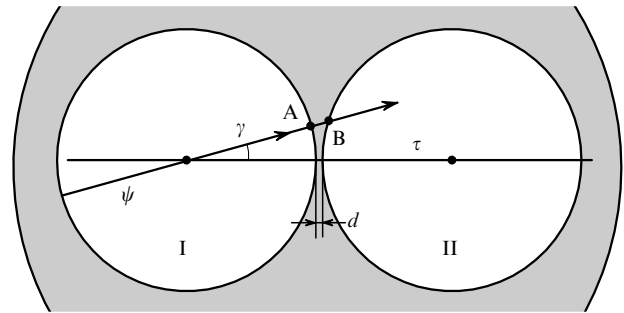


**Figure 4.** Scheme of the radiation transfer in a two-element MFC fibre for meridian beams.

It is well known that both meridian and non-meridian (skew) beams can propagate in fibres of the type shown in Fig. 4. The beams propagating at angles with respect to the fibre axes that are smaller than the critical angle  $\phi_c$  will be guided [17]. The critical angle determines the condition of total internal reflection from the silica glass-polymer interface.

It is obvious that the energy exchange between the passive and active fibres is efficient not only when they are in contact but also in the case of frustrated total internal reflection in a thin (of the order of the wavelength) polymer layer. In this case, each of the beams propagating in fibre I along a certain trajectory will have its own coefficient of power transfer to fibre II. To calculate power transfer from one fibre to another, it is necessary to find these coefficients for each of the beams and perform their summation over all the beams. Therefore, the main problem is to find the coefficients of the energy transfer from fibre I to fibre II for each of the beams.

In this paper, we consider only meridian beams, for which the interface boundaries can be assumed plane-parallel in calculations. The plane of incidence  $\psi$  of one of the meridian beams on the core-cladding interface is tilted at an angle of  $\gamma$  with respect to the plane  $\tau$  and passes through the axis of fibre I. All the meridian beams lie in planes like  $\psi$ , with different tilt angles  $\gamma$  with respect to the plane  $\tau$ . The intersection lines of the plane  $\psi$  and fibre surfaces are straight lines. The projections of these straight lines on the plane of Fig. 4 are denoted by letters A and B. It is obvious that straight lines formed by the intersection of the plane  $\psi$  with the surfaces of fibres I and II are parallel to each other. If we neglect the curvature of the silica-polymer cladding interface (which is justified for small tilt angles  $\gamma < 10^\circ$ ), the

problem of propagation of meridian beams through the region with a low refractive index (cladding) can be approximately treated as the problem of frustrated total internal reflection for the beams propagating through a plane layer of thickness  $AB$ . Note that for the diameters of passive and active fibres of  $\sim 100 \mu\text{m}$  and more, the meridian beams lying in the planes of type  $\psi$  with angles  $\gamma > 10^\circ$  will not make any noticeable contribution to radiation energy transfer at a wavelength  $\lambda \sim 1 \mu\text{m}$  from fibre I to fibre II even for  $d = 0$  because of a too large distance  $AB$ .

Based on the wave approach and Maxwell's equations, the author of paper [18] obtained for the first time the transmission coefficients for the TE- and TM-polarised light in the case of frustrated total internal reflection for plane-parallel interfaces for a layer of an arbitrary thickness. Later (see, for example, [19]), the same relations were obtained quantum-mechanically.

The transmission coefficients  $T$  for the TE (the vector  $\mathbf{E}$  is perpendicular to the plane of incidence) and TM polarised waves are described by the expressions [18]

$$T_{\text{TE}} = \frac{4 \cos^2 \theta (\sin^2 \theta - n_1^2)}{(1 - n_1^2)^2 \sinh^2 u + 4 \cos^2 \theta (\sin^2 \theta - n_1^2)},$$

$$T_{\text{TM}} = \frac{4n_1^4 \cos^2 \theta (\sin^2 \theta - n_1^2)}{(1 - n_1^2)^2 (\sin^2 \theta - n_1^2 \cos^2 \theta) \sinh^2 u + 4n_1^4 \cos^2 \theta (\sin^2 \theta - n_1^2)},$$
(1)

where

$$u = \frac{2\pi h}{n_1 \lambda} \sqrt{\sin^2 \theta - n_1^2};$$

$\theta$  is the angle of incidence;  $n_1$  is the refractive-index ratio for media with the lower and higher refractive indices;  $\lambda$  is the wavelength; and  $h$  is the thickness of a layer with a low refractive index.

The transmission coefficients for the TE- and TM-polarised meridian beams in an MFC fibre in the plane interface approximation are described by expressions (1). In this case, the angle  $\theta$  is the angle between the beam propagation direction and the normal to the fibre surface at the point of incidence. For all the meridian beams, the angle  $\theta$  lies in planes similar to the plane  $\psi$ . To simplify the notation, we introduce the angle  $\phi = 90^\circ - \theta$  (the angle between the fibre axis and beam propagation direction). The value of  $h$  is the distance  $AB$ , which in the case  $\gamma < 10^\circ$  is

$$h(\gamma) = AB(\gamma) \approx 2R(1 - \cos \gamma) + d$$
(2)

with good accuracy, where  $R$  is the radius of the MFC fibre element.

Assuming that the range of angles  $\gamma$  in which power transfer is observed is sufficiently small, we can consider approximately (another approximation) that meridian beams remain meridian after passage from one fibre to another. Therefore, we can consider the propagation of meridian beams with different specified angles  $\phi$  independently of each other. The boundary intensities  $I_b(\phi)$  of meridian beams propagating at a specified angle  $\phi$  should become identical due to the energy exchange between fibres I and II during the propagation of these beams along the MFC fibre. In the case of the uniform distribution of the

power of meridian beams propagating at an angle of  $\phi$  along the azimuth, there exists a one-to-one relation between their intensity at the fibre boundary and the total radiation power  $P(\phi)$ . Based on these considerations, the radiation exchange between fibres I and II in a two-element MFC fibre can be described by a system of differential equations for the powers  $P_I(\phi, z)$  and  $P_{II}(\phi, z)$  of meridian beams in each of the fibres

$$\frac{dP_I(\phi, z)}{dz} = k(\phi)P_{II}(\phi, z) - k(\phi)P_I(\phi, z),$$
(3)

$$\frac{dP_{II}(\phi, z)}{dz} = k(\phi)P_I(\phi, z) - k(\phi)P_{II}(\phi, z),$$

where

$$k(\phi) = \frac{\tan \phi}{4\pi R} \int_{\gamma} T(\phi, \gamma) d\gamma$$
(4)

is the coupling coefficient characterising the power exchange between the beams propagating at an angle of  $\phi$  to the axis in fibres I and II;  $T(\phi, \gamma)$  is the transmission coefficient of the beam propagating at an angle of  $\phi$  as a function of the angle  $\gamma$  [ $T(\phi, \gamma)$  can be found from expressions (1) and (2)].

By supplementing the system of equations (3) by the initial conditions, we can obtain solutions as the dependences of the power of the beams propagating at a certain angle to fibres I and II on the coordinate  $z$ . To obtain the coordinate dependence of the total radiation power propagating along fibres I and II, it is necessary to integrate the obtained solutions over all possible angles  $\phi$  and perform calculations for both polarisations. It should be taken into account in this case that the initial conditions for the beams propagating at different angles  $\phi$  will be different and dependent, generally speaking, on the excitation conditions. The initial conditions in the calculation presented below were found from the experimentally measured dependences of the far-field radiation intensity distribution.

Expressions (2)–(4) can be easily generalised to fibres I and II of different diameters. In addition, the system of equations (3) can be transformed to calculate MFC fibres with the number of elements in the first cladding above two.

Note that in the general case the absorption length of pump radiation from the first cladding ( $L_1$ ) of the MFC fibre is always greater than this length ( $L_0$ ) in a conventional double-clad fibre with the same core diameter and the same first-cladding area ( $L_1 > L_0$ ). By introducing into the second equation of system (3) the term  $\alpha_{\text{clad}}$  responsible for the absorption of pump radiation in the active fibre (in the absence of the passive fibre), we can easily show that the absorption length in the MFC fibre increases insignificantly compared to a conventional fibre if the coupling coefficient is much greater than one fourth of the absorption coefficient in the active fibre [ $k(\phi) \gg \alpha_{\text{clad}}/4$ ] or, which is the same, if the coupling length is much smaller than the absorption length ( $L_c \ll L_0$ ). Thus, the rate of the energy transfer between elements of the MFC fibre imposes the restriction on the growth of the absorption coefficient for pumping from the passive fibre, and thereby on a decrease in the laser length. In the absorbing MFC fibre, this will change absorption and the efficiency of the energy transfer along the fibre length because the beams propagating at smaller angles will be weakly absorbed.

Figure 5 shows the dependences of the coupling coefficient  $k$  on the angle  $\phi$  for MFC fibres with different parameters. One can see that the coefficient  $k$  decreases with increasing  $d$  and  $R$ , and this occurs especially rapidly at small propagation angles. The curves in Fig. 5 allow one to estimate the dependence of the beam absorption in the fibre on its propagation angle  $\phi$  and the MFC fibre parameters.

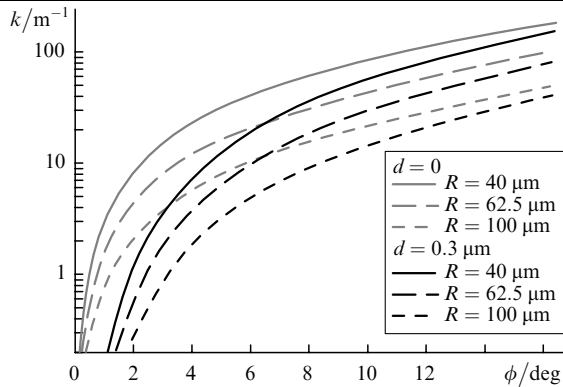


**Figure 5.** Calculated dependences of the coupling coefficient  $k$  on the angle  $\phi$  for MFC fibres with different values of  $d$  and  $R$ .

Although the above consideration concerned only meridian beams, it seems that such an approach can be also used to describe qualitatively the energy transfer in all guided beams.

#### 4. Experimental measurement of the coupling length in two-element MFC fibres

We studied two-element MFC fibres with the first-cladding ( $n = 1.45$ ) element diameters  $D_{\text{clad}} = 115 - 140 \mu\text{m}$  (depending on a sample). The reflecting polymer cladding had the refractive index  $n = 1.39$ , providing the numerical aperture for radiation in the first cladding  $\text{NA} \approx 0.4$ .

MFC fibres were excited by a pump source based on separate  $\sim 1\text{-}\mu\text{m}$  laser diodes and the numerical aperture  $\text{NA} < 0.4$ . The radiation was coupled only into fibre I (see Fig. 4), and the output power and the far-field angular radiation intensity distribution were measured for both fibres. The lengths of fibres under study were varied from 3 to 320 cm. To avoid the effect of radiation absorption in the active fibre core on the measurements, we used the emission wavelengths outside the absorption bands of active ions.

All the measurements were performed with freely lying fibres with the radii of curvature no less than 10 cm. For lower radii of curvature or in the case of external perturbations of fibres (compression, stretching, twisting, etc.), the power transferred from one element of the first cladding of the MFC fibre to another could increase significantly (over fibre pieces up to 10 cm) or decrease (probably due to a change of the contact between fibres).

Figure 6 shows the experimental dependences of the far-field angular distributions of radiation intensity from fibres I and II for several MFC fibre lengths. The results concern one MFC fibre sample with the diameter of each of the elements  $D_{\text{clad}} = 115 \mu\text{m}$  and were obtained by successively reducing the fibre length. One can see that the radiation power propagating at large angles is equalised in fibres I and

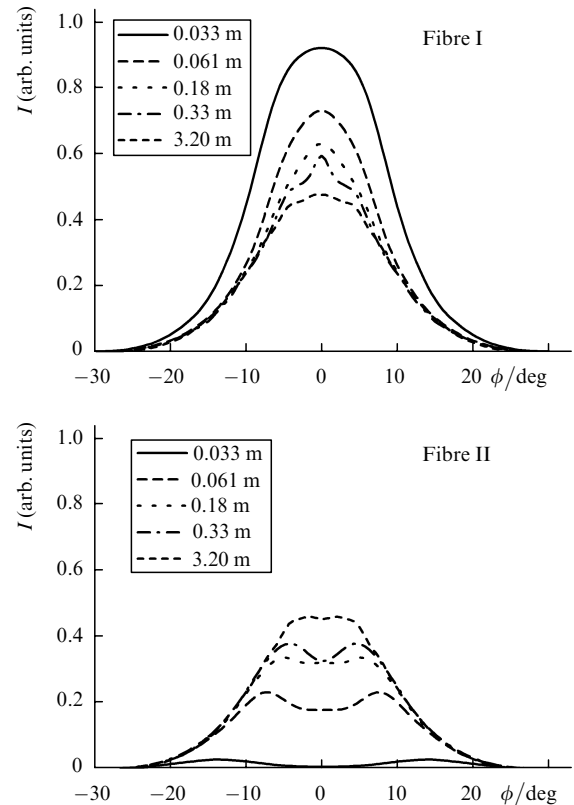


**Figure 6.** Experimental far-field angular radiation intensity distributions at the outputs of fibres I and II measured for MFC fibres of different lengths.

II much faster than the radiation power propagating at small angles. Thus, the radiation power propagating at angles greater than  $14^\circ$  is equalised already at a distance of 6 cm, while the hole at the centre corresponding to low-aperture beams is preserved at much greater distances.

Figure 7 shows the dependences of the ratio of the output power of fibre II to the total power on the MFC fibre length for the beams propagating at certain angles. One can see that the experimental data and the curves calculated for the two-element fibre with  $D_{\text{clad}} = 115 \mu\text{m}$  for  $d = 0.3 \mu\text{m}$  are in good agreement except the results obtained for a short fibre (33 mm) and the angle  $\phi = 2^\circ$ . The difference between

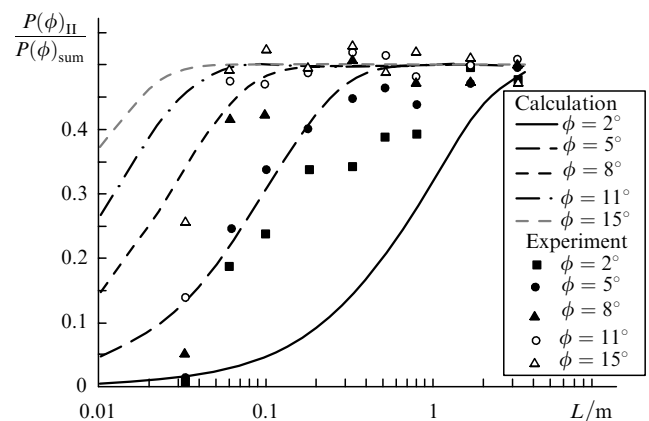


**Figure 7.** Calculated (for  $d = 0.3 \mu\text{m}$ ) and experimental ratios of the radiation power in fibre II to the total radiation power as functions of the MFC fibre length for different angles  $\phi$ .

calculations and experiment for a fibre of length 33 mm was observed not in all fibres and varied from sample to sample. In some samples, these differences were observed at a length of up to 100 mm, and in some cases at larger lengths. Such a discrepancy can be explained by the fact that the distance  $d$  between the elements of the first cladding changes over the fibre length and from sample to sample. However, because such discrepancies were observed in most samples at small lengths (shorter than 100 mm), we can conclude that these inhomogeneities are revealed over a limited length (up to a few centimetres) and have no effect on power transfer in sufficiently long (longer than 1 m) fibres. A substantial difference between the experimental data and calculations for the beams propagating at the angle  $\phi = 2^\circ$  can be explained by the fact that only meridian beams are considered in calculations, which can substantially underestimate the efficiency of the power transfer between fibres at small angles  $\phi$  and nonzero values of  $d$ .

Figure 8 shows the dependences of the ratio of the output power of fibre II integrated over all the angles to the total radiation power coupled into the fibre for the same MFC fibre pieces as in Figs 6 and 7. The calculation was performed for five values of the parameter  $d$ . As in Fig. 7, a considerable discrepancy between the experimental and theoretical power transfer efficiencies is observed only for the fibre of length 33 mm. According to Fig. 8, for the fibre of this length, an averaged distance between the elements of the first cladding is  $1.5 \mu\text{m}$ , while for the other fibre pieces, as in the previous case, the best agreement with experiment is achieved for  $d = 0.3 \mu\text{m}$ . As follows from Fig. 8, the coupling length at large distances  $d$  (of the order of micron and larger) can exceed 10 m, so that it will be difficult to use such fibres in fibre lasers and amplifiers because of a substantial decrease in absorption of pump radiation from the first cladding.

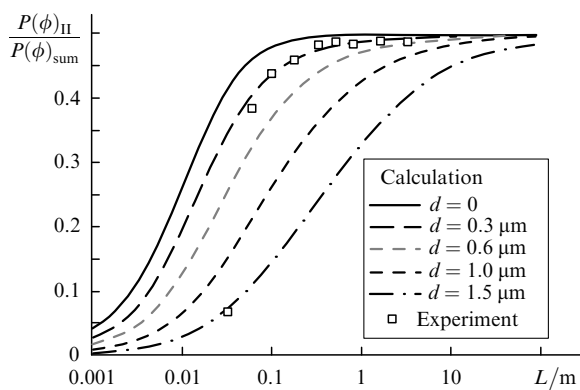


**Figure 8.** Calculated and experimental ratios of the radiation power in fibre II integrated over all angles to the total radiation power as functions of the MFC fibre length for different distances  $d$  between fibres.

According to Fig. 8, the coupling length for the given MFC fibre is  $L_c \approx 30 \text{ cm}$ . The same values of  $L_c$  were obtained for most of the two-element MFC fibres studied. Thus, we can claim that for 100-W laser with the effective pump absorption length of 22 m the condition  $L_c \ll L_0$  is fulfilled with a large safety margin.

Note that the parameter  $d = 0.3 \mu\text{m}$ , obtained after a comparison of the experimental data and calculations, can

differ from the real gap. The nonzero value indicates that the gap between elements in the MFC fibre exists and can vary over the fibre length. Such an approach allows one to simulate qualitatively the energy transfer between elements in MFC fibres and to study the dependence of the energy transfer efficiency on different parameters. We have failed to measure directly the value of  $d$  in our MFC fibres due to the smallness of this parameter and difficulties encountered in measurements through a double polymer cladding.

In the model described above we have used a number of substantial assumptions simplifying the calculation of the energy transfer between elements in an MFC fibre. Nevertheless, the agreement observed between the experimental data and calculations suggests that these assumptions are reasonable, and our model can be used for the qualitative description of the radiation transfer between elements in the MFC fibre.

## 5. Conclusions

The following conclusions can be made based on our study. Radiation powers in fibres I and II are equalised substantially nonexponentially and this process depends on the aperture of propagating radiation. The radiation power propagating in an MFC fibre at smaller angles is equalised between the elements of the MFC fibre slower than the power of radiation propagating at larger angles. Thus, to provide the efficient radiation transfer between fibres I and II, the aperture of the MFC fibre should have the maximum filling. In the case of excitation of the entire numerical aperture (0.4) in most of the two-element MFC fibres studied, the length at which powers in fibres are equalised was  $\sim 30 \text{ cm}$  within the experimental error ( $\sim 5\%$ ).

The model proposed for describing the energy transfer between the elements of the MFC fibre allows one to calculate approximately the energy transfer efficiency as a function of different parameters. The results of calculations agree qualitatively with the experimental data. A considerable discrepancy between the experimental data and calculations observed for some MFC fibre pieces of a small length (up to 10 cm) can be explained by variations in the gap between elements in the MFC fibre. In most of the samples, these variations are local and almost do not affect the power transfer between fibres I and II in MFC fibres of a large length ( $\sim 1 \text{ m}$  and longer). The presence of such regions is probably caused by technological reasons.

The all-fibre cw single-mode ytterbium-doped fibre laser with an output power of 100 W has been fabricated based on a three-element MFC fibre. It has been shown that a finite energy transfer length in the MFC fibre is not a limiting factor for this laser. The pump scheme realised in the laser demonstrates the possibilities of increasing the output power of fibre lasers and shows that MFC fibres are promising for applications in high-power fibre lasers and amplifiers.

**Acknowledgements.** The authors thank A.N. Gur'yanov, M.V. Yashkov (ICHPS RAN) and O.I. Medvedkov (FORC RAN) for their help in experiments and valuable consultations and K.S. Kravtsov (FORC RAN) for useful discussions.

## References

1. Dominic V., MacCormack S., Waarts R., et al. *Electron. Lett.*, **35**, 1158 (1999).
2. Nilsson J., Sahu J.K., Jeong Y., et al. *Proc. OFC'2005* (Anaheim, CA, 2005) OTuF1.
3. Machewirth D., Khitrov V., Samson B., et al. *Proc. OFC'2005* (Anaheim, CA, 2005) OTuF2.
4. Jeong Y., Nilsson J., Sahu J.K., et al. *Opt. Lett.*, **30** (5), 459 (2005).
5. Snitzer E., Po H., Hakimi F., et al. *Proc. Conf. Optical Fiber Sensors* (New Orleans, LA, 1988) PD5.
6. Muendel M., Engstrom B., Kea D., et al. *Proc. CLEO'97* (OSA, Washington, DC, 1997) CPD30.
7. Hakimi F., Hakimi H. *Proc. CLEO'2001* (Baltimore, MD, USA, 2001) CTUD2.
8. Kosterin A., Temyanko V., Fallahi M., Mansuripur M. *Proc. OFC'2005* (Anaheim, CA, 2005) OTuF6.
9. Karpov V.I., Dianov E.M., Kurkov A.S., et al. *Proc. OFC'99* (San Diego, CA, 1999) WM3-1.
10. Bufetov I.A., Bubnov M.M., Mel'kumov M.A., et al. *Kvantovaya Elektron.*, **35**, 328 (2005) [*Quantum Electron.*, **35**, 328 (2005)].
11. Grudin A.B., Turner P.W., Codemard C., et al. *Proc. ECOC'2002* (Copenhagen, Denmark, 2002) PD1.6.
12. Sahu J.K., Jeong Y., Algeria C., et al. *Proc. ASSP'2004* (New Mexico, 2004).
13. Muendel M. *Proc. Conf. Lasers and Electro-optics* (OSA, Washington, DC, 1996) CTuU2.
14. Liu A., Ueda K. *Opt. Commun.*, **132**, 511 (1996).
15. Mel'kumov M.A., Bufetov I.A., Kravtsov K.S., et al. *Kvantovaya Elektron.*, **34**, 843 (2004) [*Quantum Electron.*, **34**, 843 (2004)].
16. Unger H.-G. *Planar Optical Waveguides and Fibres* (Oxford: Clarendon Press, 1977; Moscow: Mir, 1980).
17. Snyder A., Love G. *Optical Waveguide Theory* (London: Chapman & Hall, 1996; Moscow: Radio i Svyaz', 1987).
18. Hall E. *Phys. Rev. (Ser. I)*, **15**, 73 (1902).
19. Lee B., Lee W. *J. Opt. Soc. Am. B*, **14** (4), 777 (1997).